Preparation and Properties of Chitosan-*graft*-Poly(methyl methacrylate) Nanoparticles Using Potassium Diperiodatocuprate (III) as an Initiator

Zhanjun Liu,[1,2] Guodong Zhao,[3] Jiugao Yu,[2] Jinqiu Zhang,[1] Xiaofei Ma,[2] Gang Han[1]

[1]*Department of Pharmaceutics, North China Coal Medical University, Tangshan 063000, China*
[2]*Department of Chemistry, School of Science, Tianjin University, Tianjin 300072, China*
[3]*Affiliated Hospital, North China Coal Medical University, Tangshan 063000, China*

Received 22 August 2009; accepted 15 September 2010
DOI 10.1002/app.33436
Published online 4 January 2011 in Wiley Online Library (wileyonlinelibrary.com).

ABSTRACT: Graft copolymer nanoparticles prepared from chitosan (CS) and methyl methacrylate (MMA) monomer were synthesized in aqueous solution by using potassium diperiodatocuprate [Cu(III)] as an initiator and characterized in terms of particle size, zeta potential, transmission electron microscopy (TEM), Fourier transform infrared spectroscopy, thermal stability, and X-ray diffraction spectrometry. The results indicated that CS was covalently linked to poly(methyl methacrylate) (PMMA), and the resulting copolymers formed nanoparticles. These nanoparticles [prepared at 35°C, in a weight ratio of MMA/CS of 5 : 1 and with a Cu(III) concentration of 1.5×10^{-3} mol/L] were 54–350 nm in size, with a mean hydrodynamic diameter of 183 ± 3 nm and were highly uniform in particle-size distribution, with a rather spherical shape and an obvious positive charge surface. The effect of reaction conditions such as Cu(III) concentration, reaction temperature, and the weight ratio of MMA/CS on the mean particle size was also investigated. Insulin-loaded nanoparticles were prepared, and their maximal association efficiency was up to 85.41%. The experiment of release *in vitro* showed that the nanoparticles gave an initial burst release followed by a slowly sustained one. © 2011 Wiley Periodicals, Inc. J Appl Polym Sci 120: 2707–2715, 2011

Key words: graft copolymers; nanotechnology; polysaccharides; potassium diperiodatocuprate; methyl methacrylate

INTRODUCTION

Chitosan (CS), a polyaminoglucose obtained by alkaline deacetylation of chitin, has interesting structure and appealing intrinsic properties that give rise to applications in many fields such as biomedicine, waste-water treatment, functional membranes, and flocculation. Especially, it has been widely used in pharmaceutical research and industry as a carrier for drug delivery and as biomedical material because of its extraordinary properties, such as biocompatibility, biodegradability, nontoxicity, adsorption properties, film-forming ability, bioadhesivity, antimicrobial activity against fungi, bacteria, and viruses.[1–5] In the recent years, CSs have been prepared nanoparticle drug-delivery systems, which can greatly prolong drug duration in blood stream and show controlled-release properties and improve the utility of drugs and reduce toxic side effects.[1] It is very difficult to control drug release for native CS nanoparticles, so that all sorts of modified CS nanoparticles have been investigated.

Correspondence to: J. Yu (kevin.tju.cn@gmail.com).

Journal of Applied Polymer Science, Vol. 120, 2707–2715 (2011)

So far, CS nanoparticles are prepared mainly by five methods: coacervation (precipitation) method,[6] emulsion-droplet coalescence method,[7] ionic-gelation method,[8] reverse micellar method,[9] and polymeric micelle method.[10,11] Among them, polymeric micelle method is usually used. Most of the approaches in the synthesis of modified nanoparticles have been applied to the synthesis of amphiphilic copolymers. There have been many reports of hydrophobic modifications of CS and nanoparticle formation by self-aggregation in aqueous solution.[12–15] These modifications can be used to synthesize CS amphiphilic polymers through introducing hydrophobic groups into CS. In the aqueous phase, the hydrophobic segments constitute a hydrophobic core of self-assembled nanoparticles surrounded by external shells. Thus, the internal core can serve as a depot for hydrophobic drugs. In addition, the plasma half-time of intravenously injected nanoparticles can be relatively prolonged because of limited uptake by the liver and spleen. Reduction in uptake by the liver and spleen has been applied to the treatment of solid tumors, because the prolonged circulation of nanoparticles allows them to accumulate and extravasate within tumor tissue.[16–18] CS can be modified and changed into amphiphilic molecule by

hydrophobic reagents, such as linoleic acid,[19] linolenic acid,[20] *N*-acetyl histidine,[21] *N*-succinyl,[22] cholesterol,[23] oleoyl,[24] and *N*-phthaloyl.[25] The hydrophobically modified polymers can self-assemble into unique nanoparticles with a hydrophobic core and a hydrophilic shell. Modification of CS can be achieved via acylation, *N*-phtaloylation, tosylation, alkylation, *O*-carboxymethylation, and *N*-carboxyalkylation.

Graft copolymerization is one of the approaches to chemical modification. Grafting vinyl polymers onto CS are usually carried out through free-radical initiators such as azobisisobutyronitrile, iron(II)-hydrogen peroxide, and transition-metal ions. The transition-metal ions commonly used for initiating graft copolymerization are Ce(IV), Mn(III), Cr(VI), Co(III), Fe(III), and Cu(II).[26–29] Among these, ceric ammonium nitrate, potassium persulfate, and ammonium persulfate (APS) are usually chosen to produce CS graft copolymer.

In the previous study of our group, graft copolymers having high grafting efficiency and percentage have been obtained by using potassium diperiodatocuprate [Cu(III)] as an efficient redox initiator. Moreover, the graft copolymerization can be carried out at a mild temperature of 35–40°C.[30,31] Few literatures have reported to directly produce CS graft copolymer nanoparticles via free-radical polymerization.

The purpose of the present work was to investigate the possibility of producing CS-*graft*-poly(methyl methacrylate) (CS-*g*-PMMA) copolymer nanoparticles using Cu(III) as an initiator and the effect of preparation conditions such as the Cu(III) concentration, reaction temperature, and weight ratio of MMA/CS on nanoparticle size. The physicochemical properties of these nanoparticles were analyzed by Fourier transform infrared spectroscopy (FTIR), transmission electron microscopy (TEM), zeta potential analysis, thermal stability, and X-ray diffraction spectrometry. Insulin-loaded nanoparticles were prepared to further investigate the properties of these nanoparticles as carriers for the drug delivery. Their association efficiency (AE) and *in vitro* release were measured. This information will be useful for further applications of Cu(III) in grafting all sorts of vinyl polymers onto natural polymers, such as starch, cellulose, CS, and keratin, to produce nanoparticles as carriers for the drug delivery.

EXPERIMENTAL

Materials

Water-soluble CS with an M_r = 6 kDa was purchased from Yuhuan Ocean Biochemical Co. (Zhejiang, China), and the degree of deacetylation was 0.93. Methyl methacrylate (MMA) from Tianjin Xintong Chemical Reagent Station (Tianjin, China) was purified by repeated washing with 4% aqueous NaOH solution, washed with distilled water to make it free from alkali, and then distilled under reduced pressure. Porcine insulin (26 IU/mg) was purchased from Xuzhou Wanbang Biochemical Co. (Jiangsu, China). All the other reagents, including KOH, $K_2S_2O_8$, KIO_4, $CuSO_4$, acetone, and NaOH, were analytical grade and used without any further purification.

Preparation and measurement of Cu(III)

Cu(III) was synthesized and measured according to the reported procedure.[32] Briefly, a mixed solution of certain amounts of KOH, $K_2S_2O_8$, KIO_4, $CuSO_4$, and distilled water (250 mL) was prepared by stirring and then heated to boiling for 1 h. The solution was cooled to room temperature and then cooled with ice to remove K_2SO_4. The carmine solution of Cu(III) was obtained after filtration with G4 filter. The concentration of Cu(III) was determined with a UV–vis spectrophotometer (Spectronic-20, model Genesys, USA) at a wavelength of 414 nm.

Preparation of CS-*g*-PMMA nanoparticles

CS-*graft*-poly(methyl methacrylate) CS-*g*-PMMA nanoparticles were obtained by radical graft copolymerization of MMA in CS solution as described below. Given amounts of CS were first dissolved into 100 mL of deionized water without addition of acetic acid, and then the required amount of the MMA was added. The pH of the solution was adjusted to 11.0 by the careful addition of 5% NaOH solution. The solution was degassed by passing nitrogen gas for 30 min to remove the dissolved oxygen under stirring and then was heated to desired temperature in an isothermal water bath. It was stirred at a speed of 300 rpm and purged with nitrogen. Subsequently, a quantity of Cu(III) initiator (6–18 mL) was dripped into the solution, and the polymerization was immediately started. After 2 h, a dispersion of the CS-*g*-PMMA nanoparticles in aqueous solutions was obtained. The obtained nanoparticles were dialyzed in demineralized water for 48 h through a semipermeable membrane with an exclusion size of 10 kDa (Dialysis Tubing-Visking, Medicell, London, UK) and then lyophilized. The weight grafting percentage (GP) was calculated as $GP = [(W_2 - W_1)/W_1] \times 100$, where W_1 and W_2 represent the weights of CS and graft CS derivatives, respectively.[30]

Measurements and analytical characterization

FTIR analysis

The IR spectra of CS and CS-*g*-PMMA nanoparticles were measured in solid state with an FTIR-8400S spectrophotometer (Shimadzu, Japan) to confirm the

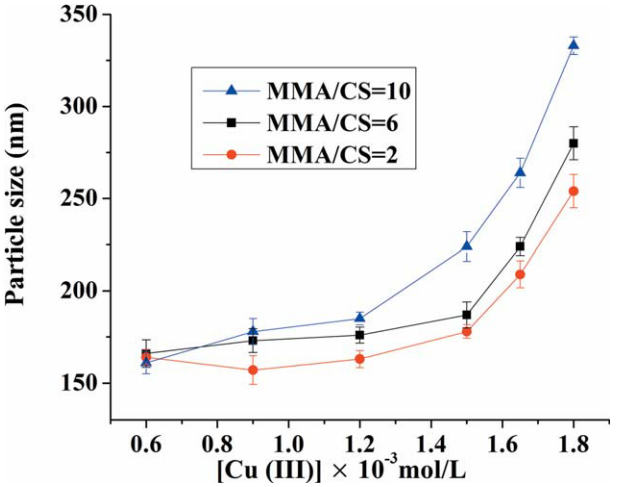

Figure 1 Effect of Cu(III) concentration on particle size. Reaction conditions: $T = 35°C$; $t = 3$ h. [Color figure can be viewed in the online issue, which is available at wileyonlinelibrary.com.]

structure of the CS-*g*-PMMA nanoparticles. The CS-*g*-PMMA nanoparticles were frozen in liquid nitrogen and lyophilized by freeze-drying. CS and nanoparticles were finely ground with KBr, respectively, and pellets were made under a hydraulic pressure of 400 kg. Spectra were scanned in the range of 4000–400 cm^{-1}.

Size and ζ-potential measurement

Fiber optic quasi-elastic light scattering (FOQELS) (Brookhaven, USA) was used to measure nanoparticle size. All FOQELS analyses were done with a 10-mW 671-nm wavelength laser diode. Particle-size measurements were carried out after equilibrating the prepared samples at 25°C. The zeta potential of the nanoparticles was measured using same instrument after calibration with BI-ZR3. Samples were diluted 50 times with 0.1 mol/L KCl and placed in the electrophoretic cell, where a potential of ± 150 mV was applied. Each sample was repeatedly measured three times.

Transmission electron microscopy

The morphology and size distribution of nanoparticles were characterized using transmission electron microscopy (TEM). Images were taken at an acceleration voltage of 80 kV using a transmission electron microscope (H-7650, Hitachi, Japan). CS-*g*-PMMA nanoparticle colloidal suspensions were sonicated for 3 min for good particle dispersion. A drop of sample solution (1 mg/mL) was placed onto a 300-mesh copper grid coated with carbon. Excess liquid was removed, and a drop of 2% (w/v) phosphotungstic acid was added on the grid for negative staining. After 2 min, the grid was tapped with filter paper to remove liquid and air-dried for TEM analysis. After the liquid on the grid being removed, the sample was then analyzed by TEM.

Thermal stability

The thermal stability of the nanoparticles was analyzed in an HCT-1 TGA (Hengjiu, China). The experiments were performed in the temperature range of 20–600°C at 10°C/min for each sample. The analysis was performed in triplicate.

X-ray diffraction

X-ray diffraction spectrometry was obtained using an XD-3A powder diffraction meter with Cu Kα radiation in the range 5°–40° (2θ) at 40 kV and 30 mA.

AE and in vitro release of insulin

To determine the association efficiency (AE) and loading content (LC) of the nanoparticles, the total amount of insulin added into nanoparticle suspensions and the amount of nonloaded insulin remaining in the clear supernatant after the loading process was measured. For this purpose, triplicate batches of nanoparticle suspensions were centrifuged at 18,000 rpm under 20°C for 30 min, and then the amount of free insulin in the clear supernatant was determined by high-performance liquid chromatography (HPLC) as described.[33] The AE and LC were calculated as follows:

$$\mathrm{AE}(\%) = (\text{total insulin amount} - \text{free insulin amount})/\text{total insulin amount} \times 100.$$

$$\mathrm{LC}(\%) = (\text{total insulin amount} - \text{free insulin amount})/\text{total nanoparticles amount} \times 100.$$

Insulin release from the nanoparticles was determined by incubating the nanoparticles in 20-mL volumes of phosphate buffer solution (PBS) of pH 6.8 at 37°C. At appropriate time intervals, the individual sample was ultracentrifuged, and the resulting filtrates were analyzed for the amount of insulin using HPLC.[34]

RESULTS AND DISCUSSION

The generation condition of nanoparticles

Effect of Cu(III) concentration

Nanoparticle preparation was conducted at different concentrations of Cu(III) and by keeping the other reaction condition constant. The influence of the concentration of Cu(III) on the particle size was shown in Figure 1. When the concentration of Cu(III)

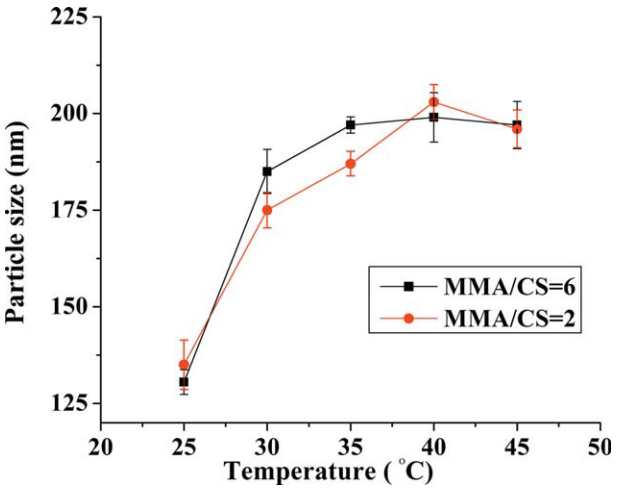

Figure 2 Effect of the reaction temperature on particle size. Reaction conditions: Cu(III) = 1.5×10^{-3} mol/L; t = 3 h. [Color figure can be viewed in the online issue, which is available at wileyonlinelibrary.com.]

was lower, the particle size changed little with increase of the concentration of Cu(III). However, the particle size would increase obviously with further increasing of the concentration of Cu(III). This behavior indicated that the free radicals on CS backbone generated by Cu(III) were little and initiated graft copolymerization at lower concentrations of the initiator. The more Cu(III) ions would lead to more graft sites on the reacted CS molecules. Thus, at higher concentrations of the initiator, the more active sites for grafting may be linked to the CS backbone, leading to the increase of the macromolecule size. Furthermore, homopolymers produced at higher initiator concentrations, which self-congregated easily, could result in increasing mean particle size. Similar observation on APS initiator was obtained by Langer.[35]

Effect of the reaction temperature

The effect of temperature was investigated by changing the reaction temperature from 25 to 45°C and keeping the other reaction condition constant. It can be seen from Figure 2 that the particle size increased with the increase of temperature at first and reached maximum value at 40°C and then decreased at higher temperatures. The increase of particle size at high temperature may be ascribed to a faster redox reaction between Cu(III) and NH_2 group of CS, generating more than one radical on every CS taking part in the copolymerization. The further decrease of particle size at higher temperature may be attributed to the termination reaction of radical resulted from higher Cu(III) concentrations fact that higher Cu(III) concentrations result in higher termination reaction of radical. The reaction temperature was lower than that of other initiators such as *tert*-butyl hydroperoxide[36] and APS.[14] The lower reaction temperature was very suitable for some biopolymers to be denatured at high temperature such as proteins and peptides.

Effect of weight ratio of MMA/CS

The influence of the ratio of MMA to CS on the particle size was shown in Figure 3. The weight ratios of MMA/CS had a significant effect on particle size. When the weight ratios were increased from 2 to 12, the particles diameters became more and more larger with 1.5×10^{-3} mol/L initiator Cu(III). This was due to two aspects. Amino groups of CS were partly positively charged. The increased diameters of nanoparticles could be due to slight aggregation caused by the reduction of surface positive charge and the consequential repulsion forces among particles. Another influence was the collision chance between free radicals and MMA. Higher weight ratio of MMA/CS increased the quantity of dispersed MMA. Nanoparticles could not be obtained with 1.7×10^{-3} mol/L initiator Cu(III) when the weight ratios were increased to 12. More dispersed MMA led to uncontrollable polymerization processes and more MMA homopolymer, which could produce some polymer floccules in addition to nanoparticles.

Effect of grafting efficiency

The grafting efficiencies of several nanoparticles prepared in different conditions were determined to assess the relationship between grafting efficiency and particle size. As shown in Figure 4, the particle

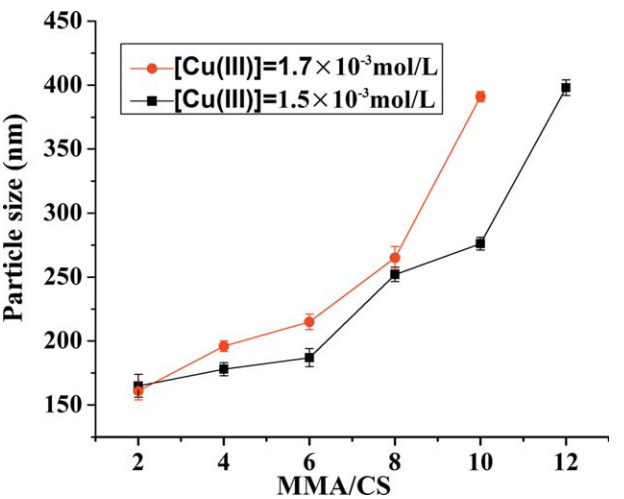

Figure 3 Effect of weight ratio of MMA/CS on particle size. Reaction conditions: T = 35°C; t = 3 h. [Color figure can be viewed in the online issue, which is available at wileyonlinelibrary.com.]

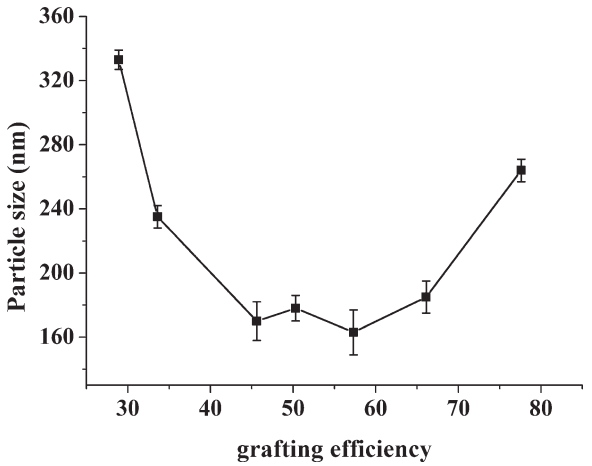

Figure 4 Effect of grafting efficiency on particle size.

size of the CS-*g*-PMMA nanoparticles was found to be impacted by grafting efficiency. The diameters of the nanoparticles reduced significantly with the increase of grafting efficiency from 28.9 to 45.6. When grafting efficiency increased from 57.3 to 77.6, the nanoparticles diameters enlarged from 163 to 265 nm. When grafting efficiency was from 45.6 to 57.3, the particles diameters minimized. The grafting efficiencies of the copolymers extracted from the transparent reaction solutions and the precipitation, which cannot yield nanoparticles in the preparation reaction, were 15.3 and 97.1, respectively.

This may be because the polymeric nanoparticles can be assembled only when the ratio of hydrophobic and hydrophilic segments were proper. That was to say, an appropriate grafting efficiency was required to ensure nanoparticles produced with a hydrophobic core surrounded by external hydrophilic shells. Increasing of hydrophilic segments with the decrease of grafting efficiency might result in an increase of sorbed water in external hydrophilic shells, leading to bigger nanoparticles. Likewise, hydrophobic cores would increase concomitantly with the increment of grafting efficiency. Nanoparticles could not form when hydrophobic segments aggregated greatly with an over high-grafting efficiency. It was so for an over-low grafting efficiency.

Reaction mechanism

There are several propositions of the grafting reaction mechanism onto CS backbone with Ce(IV) ion initiator.[37] According to the general mechanism, the complex between solvated CS and Ce(IV) ion first formated. After the dissociation of CS-Ce(IV) complex, Ce(IV) ion reduced to Ce(III), followed by the release of Ce(III) ion and pyranose ring cleavage at C2–C3 bond with the formation of a free radical on the polysaccharide backbone, which is capable of initiating graft copolymerization. The mechanism of initiation of graft copolymerization of vinyl monomers onto CS with Cu(III) as an initiator was in analogy with that of Ce(IV) ion, due to their similar redox reation. Plausible grafting and particle formation mechanisms were proposed in Scheme 1. The initiator of Cu(III) and NH_2 groups on CS combined a redox system and initiated the graft copolymerization of CS and MMA. One electron was transferred from nitrogen to Cu(III) ion, resulting in the formation of a nitrogen cation radical and a Cu(II) ion. Subsequently, the nitrogen lost a proton and generated an amino radical, which would initiate the graft

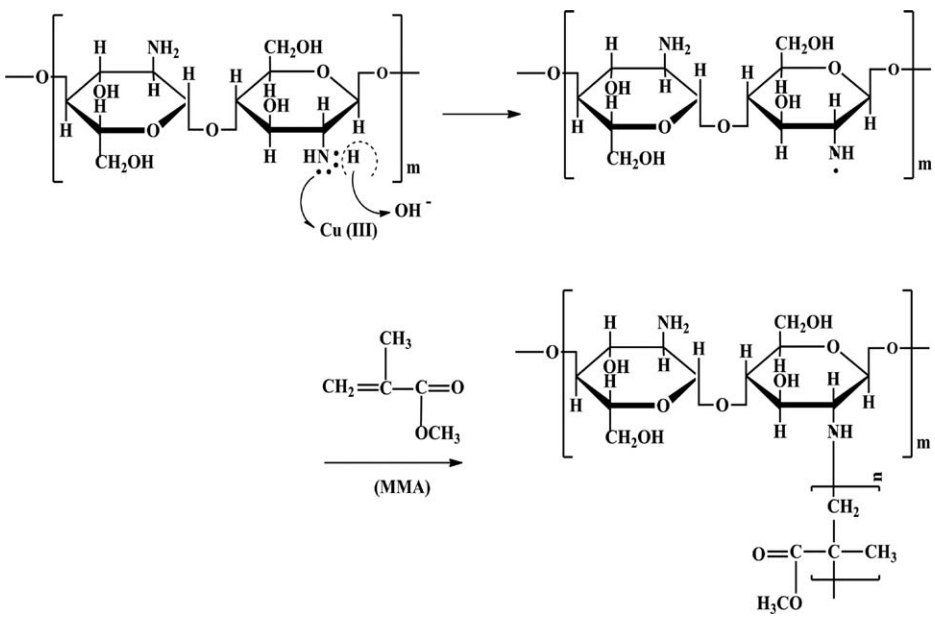

Scheme 1 An illustration for synthesis of CS-*g*-PMMA nanoparticles.

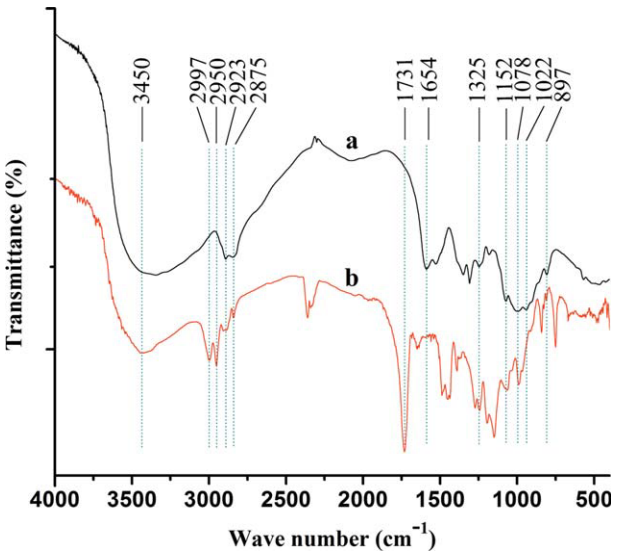

Figure 5 FTIR spectra of CS (a) and CS-*g*-PMMA nanoparticles (b). [Color figure can be viewed in the online issue, which is available at wileyonlinelibrary.com.]

copolymerization of MMA. Certainly, Cu(III) can also capture an electron from other molecule, for instance, monomer MMA, forming monomer radical, which would initiate homopolymerization of MMA.[31] The graft copolymers produced consisting of hydrophilic CS, and the hydrophobic PMMA chains would spontaneously form nanoparticles in water. The hydrophobic PMMA segment will congregate a core in the water, and the hydrophilic CS segment will coat the PMMA core to form nanoparticles. The other reason for generating nanoparticles is that CS carries obvious positive surface charges resulting in stronger repulsion between the positive chains. So the polymers could not precipitate from the solution, but form nanoparticles. The proportion of the hydrophobic segment in the grafted polymers exceeds that of the hydrophilic segment, and so the grafted polymers could form the particles in the water. In the experiment of preparation, the opalescent suspension appeared, which indicated that the nanoparticles had been formed.

FTIR spectroscopy

The Fourier transform infrared spectroscopy (FTIR) spectra of CS and CS-*g*-PMMA nanoparticles were shown in Figure 5. The IR spectrum of CS showed peaks at 1152, 1078, 1022 (related to the C—O stretching vibration), and 897 cm^{-1} assigned to the saccharide structure, and a strong characteristic amino peak at around 3400, 1654, and 1325 cm^{-1}, assigned to amide I and II bands, respectively. All these assignments were in agreement with the literature.[38] The additional sharp absorption peaks at 1731, 1150, 2997, and 2923 cm^{-1} were due to the carbonyl groups (C=O) stretching, C—O—C stretching, asymmetrical, and symmetrical stretching of the methyl groups, respectively (the absorption bands at 2950 and 2875 cm^{-1} arised from —CH_2 groups of CS). From the IR data, it can be shown that the nanoparticles had characteristic peaks of both PMMA and the saccharide of CS and its derivatives, which proved the occurrence of the grafting. The band of the hydroxyl and amino groups stretching vibrations in CS was shifted from 3400 to 3430 cm^{-1} and became clearly sharper, which was attributed to the breakup of a few hydrogen bonds after grafting.

Particle size and ζ-potential analyses

The particle size of nanoparticles was analyzed by a laser light scattering technique in aqueous solution. The particle-size distribution curves were shown in Figure 6, which displayed a narrow bimodal distribution (polydispersity index = 0.105 ± 0.038). The range of particle sizes was from 54 to 350 nm, with a mean hydrodynamic diameter of 183 ± 3 nm. The size of the majority of particles was around 187 nm. Apart from the main peak, another small peak with diameter ranging from 54 to 101 nm appeared. These small particles formed during copolymerization could be attributed to termination of two radicals resulting from uneven dispersion of Cu(III) dropping.

The nanoparticles exhibited a positive charge zeta potential in all formulations, indicating that the cationic polysaccharide CS was located on the surface of the nanoparticles while PMMA at core. Free amino groups of CS could be related to the positive zeta potential values observed. As shown in Table I, zeta potential values of nanoparticles produced from various amounts of Cu(III) concentration were approximately similar. It could be explained that the

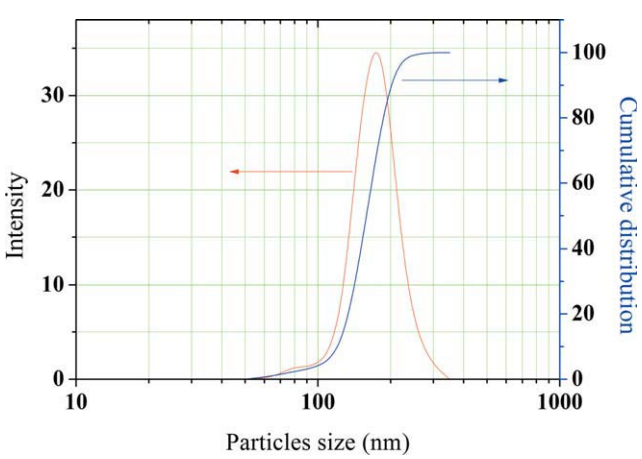

Figure 6 Size distribution of CS-*g*-PMMA nanoparticles. Preparation conditions: T = 35°C; MMA/CS = 5 : 1; Cu(III) = 1.5 × 10^{-3} mol/L; t = 3 h. [Color figure can be viewed in the online issue, which is available at wileyonlinelibrary.com.]

TABLE I
Effect of Cu (III) Concentration on the Particle Size of Nanoparticles (n = 3)

Cu(III) concentration ($/10^{-3}$ mol/L)	Zeta potential (mV)
0.6	17.7 ± 0.2
0.9	19.2 ± 0.6
1.2	19.4 ± 0.5
1.5	20.1 ± 0.2
1.8	18.4 ± 0.9

Reaction conditions: T = 35°C; MMA/CS = 5 : 1; Cu(III) = 1.5×10^{-3} mol/L; t = 3 h.

number of NH_2 groups ionized on the surface of nanoparticles did not change with increase in the ratio of surface to volume caused by the decrease of nanoparticle diameter, when fixed amount of CS was used in all formulations. This result was in agreement with the results previously obtained by Atyabi et al.[39]

Transmission electron microscopy

Negative staining transmission electron microscopy (TEM) image of nanoparticles, as shown in Figure 7, demonstrated that the shape of all nanoparticles was rather spherical and presented roughly homogeneous. All nanoparticles were separated from each other, indicating that these nanoparticles are stabilized against agglomeration by their surface charges. The mean particle diameter obtained was 115 nm [prepared at 35°C, in a weight ratio of MMA/CS of 1 : 5 and with a Cu(III) concentration of 2.0×10^{-3} mol/L], which was smaller than the size obtained by FOQELS (187 nm). The main reason was that TEM analyses were carried out in dried nanoparticles samples, whereas FOQELS determined the size using aqueous solution, and the nanoparticles were in swollen state. Similar findings were reported by Yu.[23]

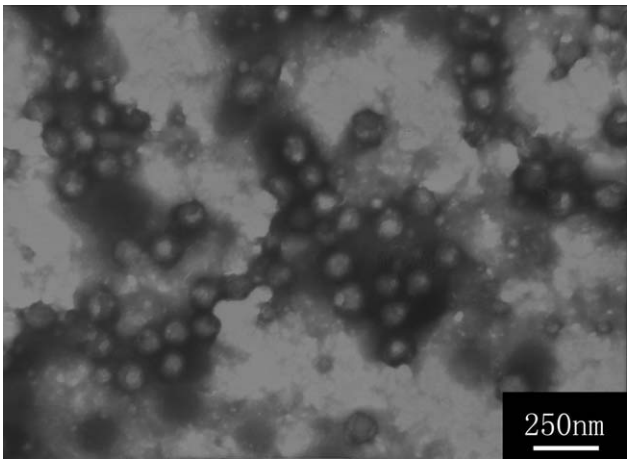

Figure 7 TEM microphotographs of CS-g-PMMA nanoparticles. Preparation conditions: T = 35°C; MMA/CS = 5 : 1; Cu(III) = 1.5×10^{-3} mol/L; t = 3 h.

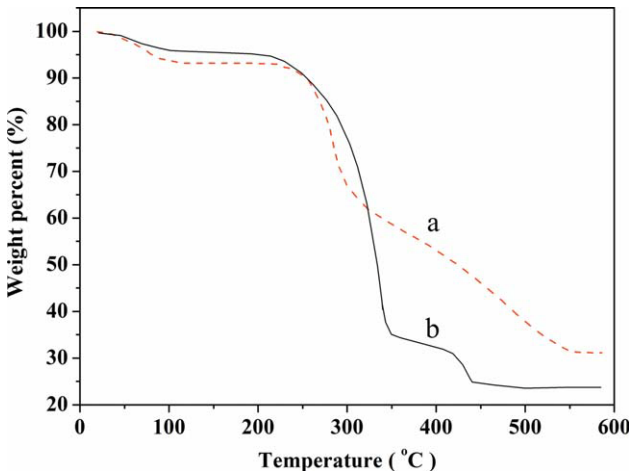

Figure 8 TGA curves of pure CS (a) and CS-g-PMMA nanoparticles (b). Preparation conditions: T = 35°C; MMA/CS = 5 : 1; Cu(III) = 1.5×10^{-3} mol/L; t = 3 h. [Color figure can be viewed in the online issue, which is available at wileyonlinelibrary.com.]

Thermal stability

The weight-loss curves were recorded at a heating rate of 10°C/min to evaluate the thermal stability of the nanoparticles. The thermograms of pure CS and CS-g-PMMA nanoparticles were shown in Figure 8. The temperature of degradation (T_d) for pure CS and nanoparticles was 226 and 217°C, respectively. Nanoparticles had higher weight percentage than CS on the same temperature under 332°C (wt % 61.9%). But nanoparticles showed a faster thermal decomposition after 332°C in comparison with that of pure CS. These results showed that the thermal stability of nanoparticles decreased slightly than that of CS, which maybe due to the breakup of the crystalline region of CS, especially by the loss of the hydrogen bonding.

Stability of nanoparticles in the solution

The nanoparticles showed a stable colloidal solution in polar solvents including 1% aqueous acetic acid even for several months without any agglomerate occurring. The positive zeta potential of the nanoparticles was maintained at 15–20 mV, which avert the nearness and aggregation of the nanoparticles, leading to an even nanoparticle suspension.

Crystallinity of nanoparticles

X-ray diffraction profiles of CS and the CS-g-PMMA nanoparticles were shown in Figure 9. The CS showed two diffraction peaks at around $2\theta = 11°$ and 21°. The diffraction intensity of nanoparticles was reduced in comparison with that of pure CS. This indicated that the ability of forming hydrogen bond of CS was decreased after forming nanoparticles. The crystalline content of CS was obviously

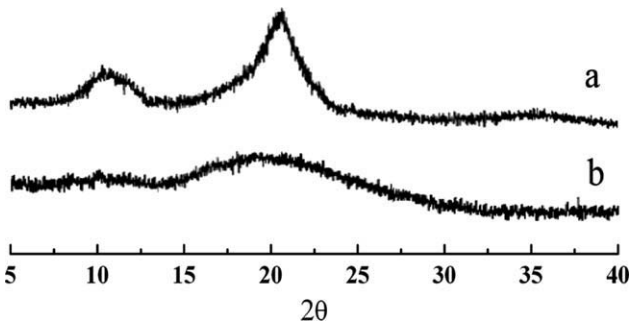

Figure 9 X-ray diffraction profiles of chitosan (a) and CS-*g*-PMMA nanoparticles (b). Preparation conditions: $T = 35°C$; MMA/CS = 5 : 1; Cu(III) = 1.5×10^{-3} mol/L; $t = 3$ h.

decreased by grafting PMMA chains into CS. Introduction of substituents into polysaccharide structures should disrupt the crystalline structure of CS, especially by the loss of hydrogen bonding.

AE and *in vitro* release of insulin

To investigate the feasibility of CS-*g*-PMMA nanoparticles as drug-delivery systems, insulin as a model drug was loaded by nanoparticles. The nanoparticles can carry insulin. One reason was that there was ionic interaction between negative insulin and positive hydrophilic chains of nanoparticles in the experiment condition. The other one was that some insulin might be encapsulated among the long hydrophilic chains in water, because the nanoparticle was covered with loose hydrophilic chains, and there would be electrostatic interaction and other interactions such as hydrogen bonding between insulin and positive hydrophilic chains of nanoparticles. So the insulin was distributed not only on the surface of the nanoparticles but also in the outer hydrophilic area.

As shown in Table II, the association efficiencies of the nanoparticles increased with the increase of the weight ratio of the nanoparticles to drug. The higher the weight ratio was, the higher the AE was. Increasing the weight ratio from 2.5/1 to 25/1 increased the AE of insulin from 36.25 to 85.41%. The LC was decreased dramatically from 14.5 to 3.42%. The association efficiencies and LC changed slightly while the weight ratio was increased from 10/1 to 25/1 and 2.5/1 to 5/1, respectively. The

TABLE II
Drug Association Efficiency and Loading Content of Insulin-Loaded Nanoparticles

Nanoparticles/drug (w/w)	Association efficiency (%)	Loading content (%)
25/1	85.41 ± 0.89	3.42 ± 0.02
10/1	80.64 ± 0.45	8.06 ± 0.01
5/1	68.39 ± 1.13	13.7 ± 0.21
2.5/1	36.25 ± 0.23	14.5 ± 0.12

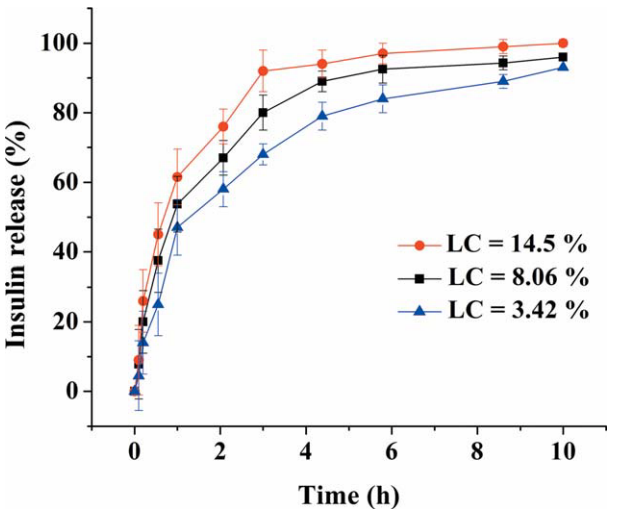

Figure 10 Insulin release profiles from CS-*g*-PMMA nanoparticles in PBS at 37°C. The results are the means ± SD ($n = 3$). [Color figure can be viewed in the online issue, which is available at wileyonlinelibrary.com.]

results were in agreement with the previous literature.[14] This could be explained that insulin was distributed into almost nanoparticles at lower weight ratio of the nanoparticles to drug; however, at higher weight ratio, there were only few insulin molecules absorbed by nanoparticles.

Figure 10 showed the *in vitro* release behavior of insulin from nanoparticles with different association efficiencies for various time intervals in PBS (pH 6.8) at 37°C. It indicated that the insulin was released in a biphasic way, that is, an initial rapid release period followed by a step of slower release. The burst effect was observed in 1 h, in which nearly 61.5%, 53.7%, and 46.9% of the drug was released from nanoparticles with LC of 14.5%, 8.06%, and 3.42%, respectively. After this initial effect, insulin was released in a continuous way for up to 10 h, reaching percentage of cumulative release close to 98%. Insulin release rate was influenced by the amount of drug loaded; a higher loading capacity provided a faster release rate. Higher levels of loaded drug lead to a wider concentration gap between the polymeric nanoparticles and the release medium, which caused a higher diffusion rate. The increase in drug content increases the amount of drug close to the surface as well as the drug in the outer hydrophilic area of nanoparticles. The former was responsible for an increased initial burst while the latter caused an increase during the induction period. The mechanism of the release was the diffusion of associated insulin from nanoparticles.

The results were coincident with the conclusion drawn by Calvo,[40] Wang,[41] and Chorny[42,43]. The opposite trend has also been reported[44–46] for various nano- and microparticulate systems. The discrepancy

occurred probably due to the different carriers and drugs used that have dissimilar release mechanism.

CONCLUSIONS

CS-*g*-PMMA nanoparticles could be successfully prepared by polymerizing MMA onto CS using Cu(III) as an initiator. The particle size was dependent on the Cu(III) concentration, temperature, and weight ratio of MMA/CS used in the nanoparticle preparation. TEM micrograph showed that CS nanoparticles had a very homogeneous morphology with predominantly spherical and uniform particles size distribution. From FTIR, X-ray diffraction, and thermal stability analysis, it was deduced that MMA could successfully be grafted onto CS and nanoparticles constituted by CS-*g*-PMMA. Model drug insulin was successfully entrapped into the CS-*g*-PMMA nanoparticles, and a high AE of insulin has been obtained, and the *in vitro* release profiles of insulin from nanoparticles show an initial burst release followed by a slowly sustained release phase. These results indicated that Cu(III) can be used to graft vinyl polymers onto natural polymer to form nanoparticles as carriers for the drug delivery. Further studies in this direction are currently in progress.

The authors thank Mr. Yemin Liu and Mrs. Wenli Zhang (Laboratory of Electron Microscopy of Laboratory Center, Northern China Coal University) for their help in the nanoparticles characterization by TEM.

References

1. Agnihotri, S. A.; Mallikarjuna, N. N.; Aminabhavi, T. M. J Control Release 2004, 100, 5.
2. Cui, F. Y.; Qian, F.; Yin, C. H. Int J Pharm 2006, 316, 154.
3. Mao, S. R.; Shuai, X. T.; Unger, F.; Simon, M.; Bi, D. Z.; Kissel, T. Int J Pharm 2004, 281, 45.
4. Kumar, M. React Funct Polym 2000, 46, 1.
5. Sarhan, A. A.; Monier, M.; Ayad, D. M.; Badawy, D. S. J Appl Polym Sci 2010, 118, 1837.
6. Mao, H. Q.; Roy, K.; Troung-Le, V. L.; Janes, K. A.; Lin, K. Y.; Wang, Y.; August, J. T.; Leong, K. W. J Control Release 2001, 70, 399.
7. Tokumitsu, H.; Ichikawa, H.; Fukumori, Y. Pharm Res 1999, 16, 1830.
8. Sonvico, F.; Cagnani, A.; Rossi, A.; Motta, S.; Di Bari, M.; Cavatorta, F.; Alonso, M.; Deriu, A.; Colombo, P. Int J Pharm 2006, 324, 67.
9. Mitra, S.; Gaur, U.; Ghosh, P. C.; Maitra, A. N. J Control Release 2001, 74, 317.
10. Jiang, G. B.; Quan, D. O.; Liao, K. R.; Wang, H. H. Mol Pharm 2006, 3, 152.
11. Jiang, G. B.; Quan, D. P.; Liao, K. R.; Wang, H. H. Carbohydr Polym 2006, 66, 514.
12. Kim, J. H.; Kim, Y. S.; Kim, S.; Park, J. H.; Kim, K.; Choi, K.; Chung, H.; Jeong, S. Y.; Park, R. W.; Kim, I. S.; Kwon, I. C. J Control Release 2006, 111, 228.
13. Kim, J. H.; Kim, Y. S.; Park, K.; Kang, E.; Lee, S.; Nam, H. Y.; Kim, K.; Park, J. H.; Chi, D. Y.; Park, R. W.; Kim, I. S.; Choi, K.; Kwon, I. C. Biomaterials 2008, 29, 1920.
14. Qian, F.; Cui, F. Y.; Ding, J. Y.; Tang, C.; Yin, C. H. Biomacromolecules 2006, 7, 2722.
15. Li, Y. Y.; Chen, X. G.; Yu, L. M.; Wang, S. X.; Sun, G. Z.; Zhou, H. Y. J Appl Polym Sci 2006, 102, 1968.
16. Brannonpeppas, L. Int J Pharm 1995, 116, 1.
17. Prabaharan, M.; Mano, J. F. Drug Delivery 2005, 12, 41.
18. Soppimath, K. S.; Aminabhavi, T. M.; Kulkarni, A. R.; Rudzinski, W. E. J Control Release 2001, 70, 1.
19. Liu, C. G.; Chen, X. G.; Park, H. J. Carbohydr Polym 2005, 62, 293.
20. Naruta, Y.; Goto, M.; Tawara, T.; Tani, F. Chem Lett 2002, 162.
21. Park, J. S.; Han, T. H.; Lee, K. Y.; Han, S. S.; Hwang, J. J.; Moon, D. H.; Kim, S. Y.; Cho, Y. W. J Control Release 2006, 115, 37.
22. Zhu, A. P.; Chen, T.; Yuan, L. H.; Wu, H.; Lu, P. Carbohydr Polym 2006, 66, 274.
23. Yu, J. M.; Li, Y. H.; Qiu, L. Y.; Jin, Y. Eur Polym J 2008, 44, 555.
24. Xing, K.; Chen, X. G.; Li, Y. Y.; Liu, C. S.; Liu, C. G.; Cha, D. S.; Park, H. J. Carbohydr Polym 2008, 74, 114.
25. Yoksan, R.; Chirachanchai, S. Bioorg Med Chem 2008, 16, 2687.
26. Laue, C.; Hunkeler, D. J Appl Polym Sci 2006, 102, 885.
27. Zohuriaan-Mehr, M. J.; Pouriavadi, A. Polym Adv Technol 2003, 14, 508.
28. Yilmaz, E.; Adali, T.; Yilmaz, O.; Bengisu, M. React Funct Polym 2007, 67, 10.
29. Arica, M. Y.; Yilmaz, M.; Bayramoglu, G. J Appl Polym Sci 2007, 103, 3084.
30. Liu, Y. H.; Liu, Z. H.; Zhang, Y. Z.; Deng, K. L. J Appl Polym Sci 2003, 89, 2283.
31. Liu, Y. H.; Bai, L. B.; Zhang, R. Y.; Li, Y. X.; Liu, Y. W.; Deng, K. L. J Appl Polym Sci 2005, 96, 2139.
32. Jaiswal, P. K.; Yadava, K. L. Indian J Chem 1973, 11, 837.
33. Simon, M.; Wittmar, M.; Bakowsky, U.; Kissel, T. Bioconjugate Chem 2004, 15, 841.
34. Lin, Y. H.; Mi, F. L.; Chen, C. T.; Chang, W. C.; Peng, S. F.; Liang, H. F.; Sung, H. W. Biomacromolecules 2007, 8, 146.
35. Langer, K.; Marburger, C.; Berthold, A.; Kreuter, J.; Stieneker, F. Int J Pharm 1996, 137, 67.
36. Li, P.; Zhu, J. M.; Sunintaboon, P.; Harris, F. W. Langmuir 2002, 18, 8641.
37. Romakevi, T.; Budrien, S.; Liubertien, A.; Gerasimik, I.; Zubrien, A. Chemija 2007, 18, 33.
38. Brugnerotto, J.; Lizardi, J.; Goycoolea, F. M.; Arguelles-Monal, W.; Desbrieres, J.; Rinaudo, M. Polymer 2001, 42, 3569.
39. Atyabi, F.; Moghaddam, F. A.; Dinarvand, R.; Zohuriaan-Mehr, M. J.; Ponchel, G. Carbohydr Polym 2008, 74, 59.
40. Calvo, P.; RemunanLopez, C.; VilaJato, J. L.; Alonso, M. J. J Appl Polym Sci 1997, 63, 125.
41. Wang, C.; Fu, X.; Yang, L. S. Chin Sci Bull 2007, 52, 883.
42. Chorny, M.; Fishbein, I.; Danenberg, H. D.; Golomb, G. J Control Release 2002, 83, 389.
43. Chorny, M.; Fishbein, I.; Danenberg, H. D.; Golomb, G. J Control Release 2002, 83, 401.
44. Avgoustakis, K.; Beletsi, A.; Panagi, Z.; Klepetsanis, P.; Karydas, A. G.; Ithakissios, D. S. J Control Release 2002, 79, 123.
45. Ruan, G.; Feng, S. S. Biomaterials 2003, 24, 5037.
46. Budhian, A.; Siegel, S. J.; Winey, K. I. Int J Pharm 2008, 346, 151.